Supporting Information

Critical Role of Al Pair Sites in Methane Oxidation to Methanol on Cu-Exchanged Mordenite Zeolites

Peijie Han[a], Zhaoxia Zhang[a], Zheng Chen[a], Jingdong Lin[a], Shaolong Wan[a], Yong Wang[b], Shuai Wang[a,*]

[a] State Key Laboratory for Physical Chemistry of Solid Surfaces, Collaborative Innovation Center of Chemistry for Energy Materials, National Engineering Laboratory for Green Chemical Productions of Alcohols-Ethers-Esters, and College of Chemistry and Chemical Engineering, Xiamen University, Xiamen 361005, China

[b] Voiland School of Chemical Engineering and Bioengineering, Washington State University, Pullman, Washington 99164, United States

* Corresponding author. Email: shuaiwang@xmu.edu.cn

1. Method for Simulation of UV-Vis Spectra

The UV-Vis adsorption simulations were performed with the Gaussian 16 program package[1], which followed a two-step procedure: (1) optimizing the ground-state geometry and (2) determining the vertical electronic transition energies by means of time-dependent density-functional theory (TD-DFT)[2]. Cluster models of the MOR 8-MR structure ($Si_{8-x}Al_xO_{24}H_{16+x}$) were built with the edge-O atoms terminated by H-atoms. During geometry optimization, terminal H atoms were allowed to relax while all other atoms were fixed. Optimization of the geometry was performed at the PBE0/6-31G(d,p) level[3] with the dispersion correction derived from the Grimme's D3BJ method[4]. Excitation spectra were obtained using the TD-DFT theory at the PBE0/def-TZVP level and were calculated for the lowest excited state. It needs to be emphasized that the TD-DFT method cannot calculate the absolute electronic spectra of species involving transition metal atoms accurately. This method is merely applied here as an affordable computing approach to estimate the relative UV-Vis band positions for the Cu-oxo clusters grafted at the Al_{pair} sites and those Cu-OH moieties grafted at the Al_{isol} sites.

2. Measurement of Infrared Spectra

Measurements of *in situ* diffuse reflectance infrared Fourier transform spectroscopy (DRIFTS) for the surface intermediates involved in methane oxidation on Cu-MOR samples were carried out on NICOLET iS50 FTIR Spectrometer (Thermo Scientific, Waltham, MA, USA). The Cu-MOR sample was first pretreated in flowing O_2 (20 mL min^{-1}) at 673 K for 1 h. After cooling to 473 K, the background spectrum was collected in flowing He (20 mL min^{-1}). A flow of methane (20 mL min^{-1}) was then introduced into the reactor cell to contact with pretreated Cu-MOR sample at 473 K for 1 h, followed by purging with He (40 mL min^{-1}) for 0.5 h at the same temperature. DRIFTS spectra were collected *in situ* within the 650-4000 cm^{-1} region (4 cm^{-1} resolution; averaged by 64 scans) and were analyzed by subtracting the measured background spectra.
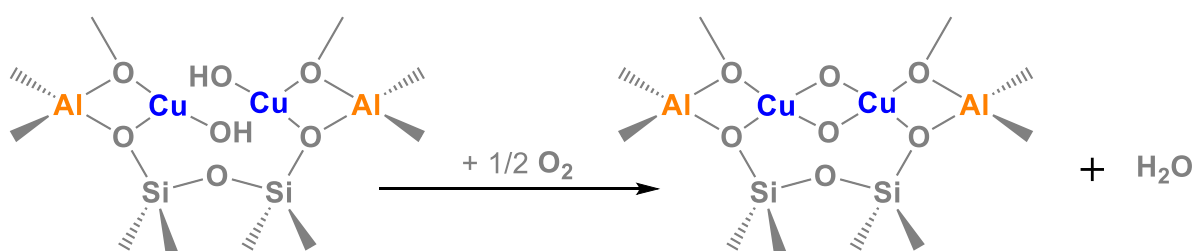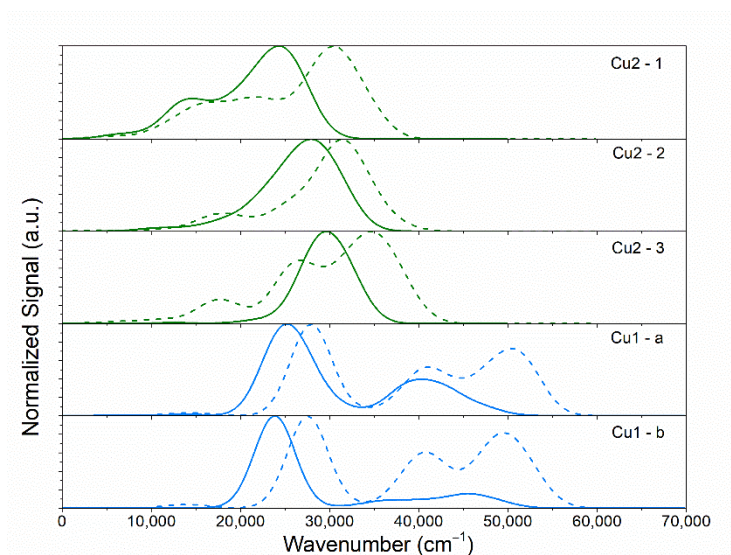
3. Results and Discussion
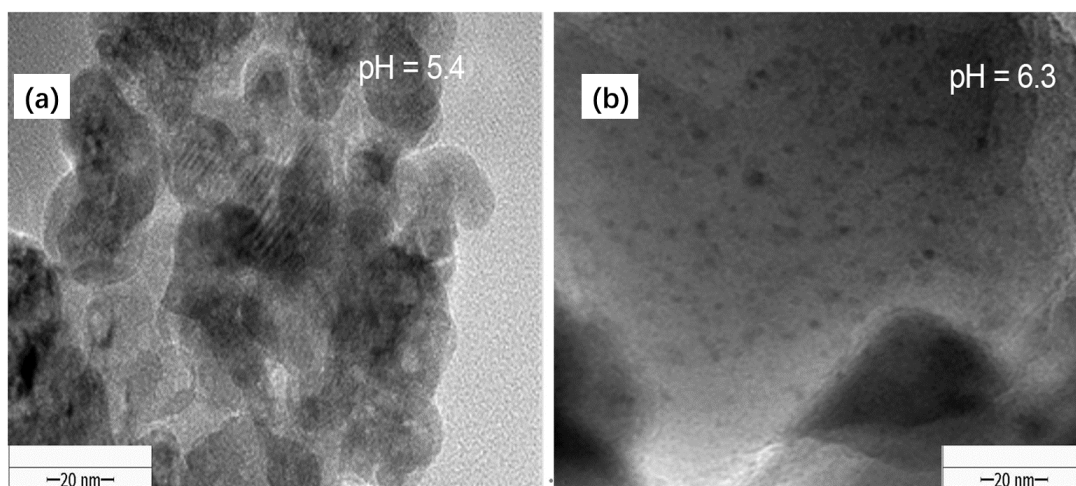
Figure S1. TEM images for the Cu-MOR-A catalyst (424 μmol_{Cu} $g_{catalyst}^{-1}$) prepared at constant pH values of (a) 5.4 and (b) 6.3.
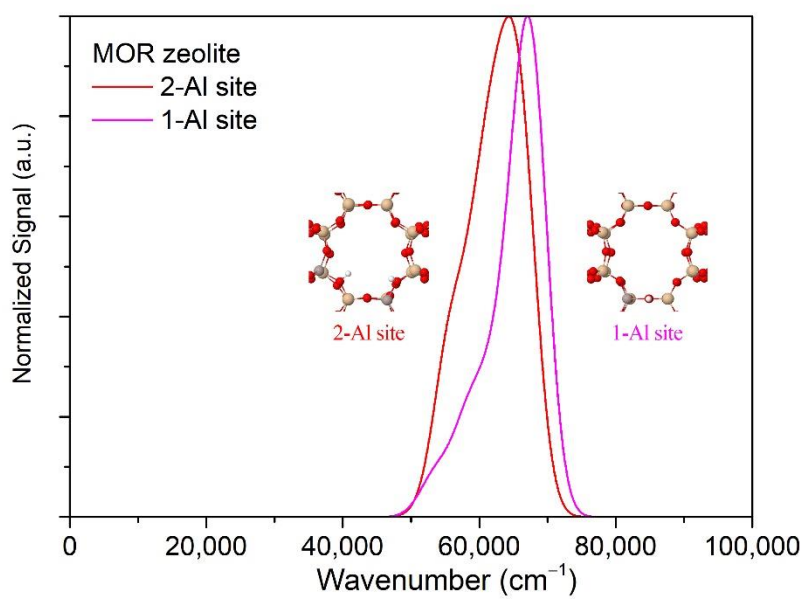
MOR (0 0 1)

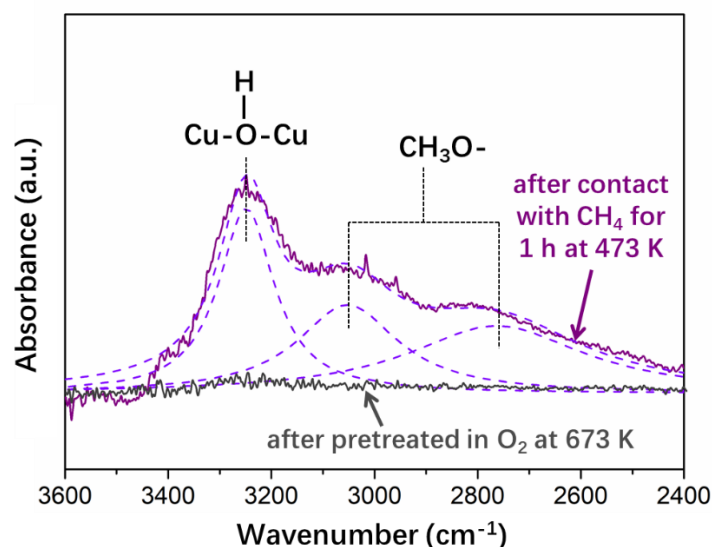**MOR (0 1 0)**
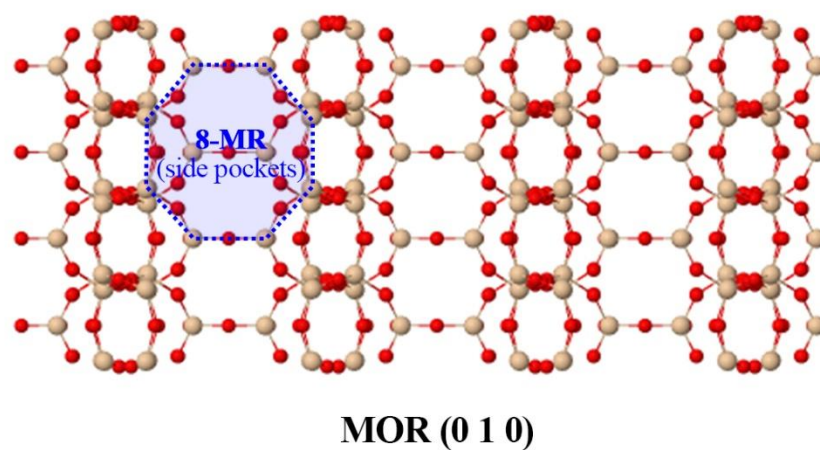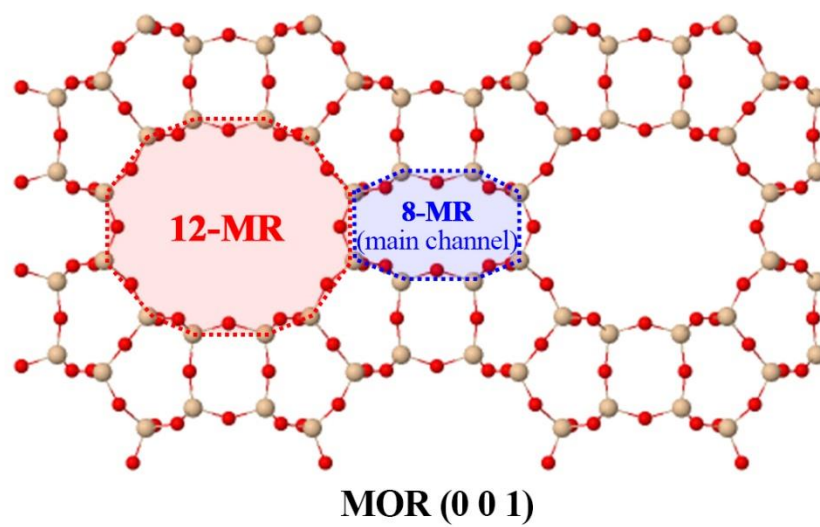
Figure S2. Illustration of the 12-MR and 8-MR motifs in MOR.

Figure S3. Formation of Cu_2O_2 clusters from two vicinal CuOH species bound to Al pair sites in MOR.

Figure S4. Predicted UV-Vis spectra of the MOR-supported Cu-oxo species before (solid) and after (dotted) reaction with methane.


Figure S5. Predicted UV-Vis spectra of the MOR zeolite structure.

Figure S6. *in situ* Diffuse reflectance infrared Fourier transform spectra for an activated Cu-MOR-A sample after the methane oxidation process at 473 K for 1 h. The Cu-MOR-A sample (174 μmol_{Cu} $g_{catalyst}^{-1}$) was preactivated in a O_2 flow at 673 K for 1 h. Dashed curves represent fitted adsorption bands obtained from signal deconvolution.

Note: As shown in Figure S6, three adsorption bands appeared within the 2400-3600 cm^{-1} region after the oxidation of methane by a Cu-MOR-A sample (174 μmol_{Cu} $g_{catalyst}^{-1}$) pre-activated in O_2 flow at 673 K, which was slightly lower than for that the activity tests of the Cu-MOR samples (723 K) due to the temperature limit of the IR cell. Specifically, the two bands centered at 2764 and 3052 cm^{-1} are attributable to the C–H stretching of formed methoxy surface species, and the band at 3249 cm^{-1} is attributable to the bonding of H atom to the bridged O of Cu-oxo species[5]. These observations are consistent with the proposed C-H dissociation of methane on the Cu-oxo species, which is regarded as a crucial step for methane activation.
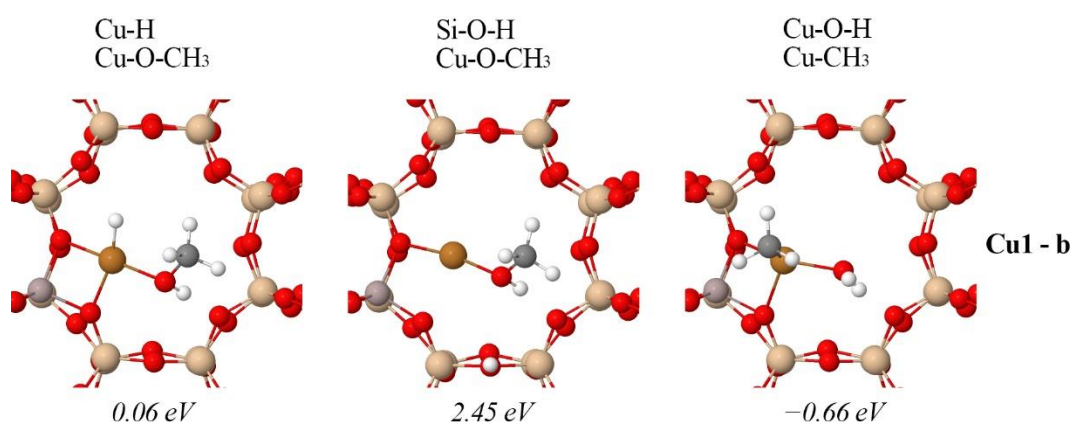
Figure S7. DFT-derived structures for Cu1-b bound with dissociated methyl and H moieties and the corresponding dissociation energy of methane.

Table S1. DFT-derived geometric parameters and charge distribution for the Cu-oxo species before and after methane dissociation onto them.

	Distance (Cu–O) /Å [a]		Angle (Cu–O–Cu) [b]		Charge (Cu) [c]		Charge (O) [d]	
	before	after	before	after	before	after	before	after
Cu1-a	1.771	2.008	-	-	1.19	0.96	−0.95	−0.92
Cu1-b	1.763	2.001	-	-	1.13	0.96	−0.91	−0.92
Cu2−1	1.811	2.238	88.8 °	74.0 °	1.10	0.96	−0.54	−0.73
Cu2-2	1.794	1.937	95.5 °	92.6 °	1.09	1.04	−0.58	−0.78
Cu2-3	1.790	1.915	99.0 °	100.8 °	1.12	1.03	−0.64	−0.80
Cu3	1.784	1.894	112.3 °	102.9 °	1.15	1.10	−0.78	−0.93

[a] Average bond length of each Cu–O bond; [b] Average bond angle of each Cu–O–Cu structure; [c] Average charge distribution of each Cu atom in the Cu-oxo species; [d] Average charge distribution of each O atom in the Cu-oxo species.

References

(1) Frisch, M. J.; Trucks, G. W.; Schlegel, H. B.; Scuseria, G. E.; Robb, M. A.; Cheeseman, J. R.; Scalmani, G.; Barone, V.; Petersson, G. A.; Nakatsuji, H.; Li, X.; Caricato, M.; Marenich, A. V.; Bloino, J.; Janesko, B. G.; Gomperts, R.; Mennucci, B.; Hratchian, H. P.; Ortiz, J. V.; Izmaylov, A. F.; Sonnenberg, J. L.; Williams; Ding, F.; Lipparini, F.; Egidi, F.; Goings, J.; Peng, B.; Petrone, A.; Henderson, T.; Ranasinghe, D.; Zakrzewski, V. G.; Gao, J.; Rega, N.; Zheng, G.; Liang, W.; Hada, M.; Ehara, M.; Toyota, K.; Fukuda, R.; Hasegawa, J.; Ishida, M.; Nakajima, T.; Honda, Y.; Kitao, O.; Nakai, H.; Vreven, T.; Throssell, K.; Montgomery Jr., J. A.; Peralta, J. E.; Ogliaro, F.; Bearpark, M. J.; Heyd, J. J.; Brothers, E. N.; Kudin, K. N.; Staroverov, V. N.; Keith, T. A.; Kobayashi, R.; Normand, J.; Raghavachari, K.; Rendell, A. P.; Burant, J. C.; Iyengar, S. S.; Tomasi, J.; Cossi, M.; Millam, J. M.; Klene, M.; Adamo, C.; Cammi, R.; Ochterski, J. W.; Martin, R. L.; Morokuma, K.; Farkas, O.; Foresman, J. B.; Fox, D. J. *Gaussian 16 Rev. B.01*, Wallingford, CT, 2016.

(2) Runge, E.; Gross, E. K. U., Density-functional yheory for time-dependent systems. *Phys. Rev. Lett.* **1984,** *52*, 997–1000.

(3) Adamo, C.; Barone, V., Toward reliable density functional methods without adjustable parameters: The PBE0 model. *J. Chem. Phys.* **1999,** *110*, 6158–6170.

(4) Grimme, S.; Antony, J.; Ehrlich, S.; Krieg, H., A consistent and accurate ab initio parametrization of density functional dispersion correction (DFT-D) for the 94 elements H-Pu. *J. Chem. Phys.* **2010,** *132*, 154104–154123.

(5) Sushkevich, V. L.; Palagin, D.; Ranocchiari, M.; van Bokhoven, J. A., Selective anaerobic oxidation of methane enables direct synthesis of methanol. *Science* **2017,** *356*, 523–527.